



Computational Studies of Thiourea Derivatives as Anticancer Candidates through Inhibition of Sirtuin-1 (SIRT1)

Ruswanto ^a, Richa Mardianingrum ^b, Arry Yanuar ^{c,*}

^a Pharmaceutical Study Program, Bakti Tunas Husada College of Health Sciences, Tasikmalaya, Indonesia

^b Pharmaceutical Study Program, Universitas Perjuangan, Tasikmalaya, Indonesia

^c Faculty of Pharmacy, Universitas Indonesia, Depok, Indonesia

*Corresponding author: arry.yanuar@ui.ac.id

<https://doi.org/10.14710/jksa.25.3.87-96>



Article Info

Article history:

Received: 7th December 2021

Revised: 28th February 2022

Accepted: 8th March 2022

Online: 31st March 2022

Keywords:

molecular dynamics; cancer;
 molecular docking; sirtuin-1;
 thiourea

Abstract

Cancer is a disease that starts from the uncontrolled growth of abnormal cells in the organs or tissues of the body, which is the second leading cause of death in the world. One of the targets in discovering and developing anticancer drugs is Sirtuin-1. SIRT1 can act as a tumor suppressor or tumor promoter depending on its target in a particular signalling pathway or on particular cancer. This study aimed to study the interaction of a thiourea derivative with SIRT1 (PDB ID:4I5I) through its inhibition of histone deacetylase. Research has been carried out in silico with molecular docking (MGLTools.1.5.6) and molecular dynamics (Desmond 2019) of three thiourea derivatives to the receptor. In addition, pharmacokinetic parameters, toxicity, and selection of Lipinski's Rule of Five were also tested. Molecular docking results showed that compound **b** ([2-(methylcarbamothioylcarbamoyl)phenyl]benzoate) had the lowest ΔG value of -9.29 kcal/mol with a KI value of 0.156 μM compared to other thiourea derivatives and was proven by molecular dynamics tests for 30 ns and amino acids that play an active role in the interaction include the residue PheA:297. In terms of pharmacokinetics and toxicity, compound **b** is better than natural ligands. Compound **b** is predicted to be used as an anticancer candidate through further research.

1. Introduction

Cancer is a general term for a large group of diseases that can affect any part of the body. Other terms used are malignant tumor and neoplasm. One of the hallmarks of cancer is the rapid creation of abnormal cells that grow beyond their usual limits. They can then invade adjacent parts of the body and spread to other organs; the latter process is called metastasis. Cancer is the leading cause of death worldwide, accounting for nearly 10 million deaths in 2020 [1]. Cancer arises from transforming normal cells into tumor cells in a multi-stage process that generally progresses from pre-cancerous to malignant tumors. These changes are the result of the interaction between a person's genetic factors and three categories of external agents, including physical carcinogens, such as ultraviolet and ionizing radiation; chemical carcinogens, such as asbestos, components of tobacco smoke, alcohol,

aflatoxins (food contaminants), and arsenic (drinking water contaminants); and biological carcinogens, such as infections from certain viruses, bacteria, or parasites [2, 3].

The SIRT1 protein is one of the Silent Information Regulator 2 (Sir2) protein members. SIRT1 has received considerable attention as an epigenetic regulator in human physiology [4]. Alteration of sirtuin expression is critical in several diseases, including metabolic syndrome, cardiovascular disease, cancer, and neurodegeneration. SIRT1 protein is an NAD⁺-dependent histone deacetylase, where the cell culture system of SIRT1 can inhibit apoptosis. Inhibition of SIRT1 or broad-spectrum sirtuin inhibitors may provide therapeutic benefits in certain types of cancer. Many SIRT inhibitory compounds, such as cambinol, sirtinol, and salermide, effectively induce cancer cell apoptosis [5]. In addition,

other studies have stated that N-methyl-thiocarbamoyl-lysine and N-carboxyethyl-thiocarbamoyl-lysine compounds have powerful inhibitory activity against SIRT1/2/3/5 [6].

Thiourea is a compound containing sulfur and nitrogen, widely used in studies as anticancer, such as nitrosourea, hydroxyurea, and 5-fluorouracil [7]. In another study, it was stated that phenylthiourea derivatives could inhibit melanin production showing strong anticancer activity against melanoma [8], and the compound N-benzoyl-N'-(4-fluorophenyl) thiourea is predicted to inhibit SIRT1 as an anticancer [9, 10, 11]. In addition, other thiourea derivatives have activity as a central nervous system depressant [12], antimicrobial [13], antitumor, and anti-inflammatory [14]. Based on density functional theory (DFT) studies, molecular docking, and molecular dynamics, it is known that thiourea derivatives provide antineoplastic effectiveness through their inhibition of protein kinases [15].

Research and drug discovery are conducted to obtain new drugs by reducing or eliminating existing side effects and increasing biological activity through molecular modification. The compound N-ethyl-N-phenylthiourea (EFTU) showed better anticancer activity against human breast cancer cells (T47D) than the comparison drug hydroxyurea. The IC_{50} value of N-ethyl-N-phenylthiourea (EFTU) was 0.74 mM, lower than hydroxyurea at 4.58 mM [16]. In addition, the compound 1,1'-(1,4-phenylene)bis(3-(benzo[d][1,3]dioxol-5-yl)thiourea) has activity on cancer cells HCT116, HepG2, and MCF-7 with a smaller IC_{50} value compared to doxorubicin as a comparison drug [17].

Several steps were conducted in drug discovery and development, including prediction of the physicochemical properties of compounds by observing their pharmacokinetic properties (ADME), toxicity, and investigating the interaction of compounds (ligands) with receptors (proteins) in silico. The molecular docking method is used to predict the binding orientation of the compound to its target protein in determining the affinity and activity of small molecules [18]. In the molecular docking study, the compound 1-(4-methoxyphenyl)-3-(pyridine-3-ylmethyl)thiourea has a binding affinity value of -7.41 kcal/mol [19]. In another study, the compound 3-(naphthalen-2-yl)-N-((1,3-difluoromethyl)phenyl)carbamooylthioylamino)-1,2,4-oxadiazole-5-carboxamide had the best potential as an inhibitor SIRT-1 with an IC_{50} value of 13 IC_{50} [20].

In previous research, researchers have researched thiourea derivatives as anticancer either in silico or in vitro [21, 22, 23]. Based on this background, the researchers modified three other thiourea-derived compounds (Figure 1) and studied their interactions with the SIRT1 protein. The in silico studies investigated pharmacokinetics, molecular docking, and molecular dynamics. Molecular docking is performed using AutodockTools because of the free, open-source software suite used in the virtual screening of small molecules to macromolecular receptors. AutoDock has been applied to various biological systems for protein-ligand binding and

prediction of binding affinity with good correlation with experimental binding affinity for several protein systems [24]. However, visualization of two-dimensional interactions must utilize other program facilities, for example, discovery studio visualizer.

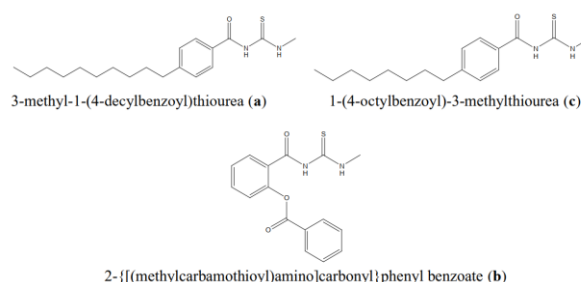


Figure 1. Structure of the design compound

2. Methods

This research was conducted in silico by performing physicochemical screening through pharmacokinetics prediction, toxicity, Lipinski's Rule of Five analysis, molecular docking, and molecular dynamics of three thiourea compounds against the SIRT1 receptor.

2.1. Equipment and Materials

The tools used in this research include computer hardware with specifications Intel® Core™ i5-6400 CPU @ 3.90 GHz (4CPUs), Nvidia Geforce GTX 970 Gigabyte OC Edition GPU, 8GB DDR4 RAM. The software was Marvin Sketch for an academic license, Molegro Molecular Viewer, MGLTools 1.5.6, Discovery Studio Visualizer, Desmond Package for an academic license, and preADMET.

The materials were 2D structures of three thiourea-derived compounds (Figure 1) drawn using the Marvin Sketch for an academic license program. SIRT1 protein was downloaded through <http://www.rcsb.org/pdb/> with PDB code 4I5I [25].

2.2. Predictive Analysis of Pharmacokinetics, Toxicity and Lipinski's Rules of Five

The screening process of the test compounds was performed to predict the physicochemical properties of the test compounds. The screening was conducted to predict pharmacokinetic properties, toxicity, and compliance with Lipinski's Rules of Five [26, 27].

2.3. Preparation of Ligands and Receptors

The ligands were drawn in two dimensions using Marvin Sketch software, then protonated to produce a pH 7.4, and then the file was saved in .mrv format. The next step was to determine the conformation of the structure by performing a conformational search with the MMFF94 force field setting. Then the file was saved in the form of mol2 [28].

The 3-dimensional structure of SIRT1 was downloaded from the Protein Data Bank website with the code PDB 4I5I and (6S)-2-chloro-5,6,7,8,9,10-hexahydrocyclohepta[b]indole-6-carboxamide as a natural ligand. SIRT1 protein was separated from ligands and water molecules using Molegro Molecular Viewer

software; consequently, only the SIRT1 monomeric protein structure was used as the target protein.

2.4. Validation of Molecular Docking Method

The method was validated by re-docking the natural ligand to the protein's active site with a grid box size of 40 x 40 x 40 Å and x, y, and z coordinates (42.194; -21,207; and 18,508 Å), and the value obtained was Root Mean Square Deviation. (RMSD) in angstroms (Å) [29]. The validation of the molecular docking method is declared valid if the RMSD value of ≤ 2 Å was obtained [30].

2.5. Docking of Test Ligand

Docking of test ligand was carried out for the same target protein on natural ligands using the Autodock program with the Lamarckian GA algorithm and without repetition with each docking yielding 100 conformations. The results seen at this stage were the value of binding free energy (BFE) or ΔG with units of kcal/mol and the value of the inhibition constant (KI) [28].

2.6. Docking Result Visualization

The interaction of ligands with receptors in 2D and 3D forms can be determined through docking results visualization. As a result, the position of the ligand-receptor conformation with the lowest BFE was obtained, and a complex file was created in the (.pdb) format for visualization using the Discovery Studio Visualizer software.

2.7. Molecular Dynamics Analysis

Molecular dynamics studies were carried out on one of the best compounds resulting from molecular docking and natural ligands for 30 ns using the Desmond software for academic license (DE Shaw Research, New York) program to examine the bond stability of the ligand-4I5I complex. The simulation system used a TIP3P water model and 0.15 M NaCl to mimic a physiological ionic concentration. Energy minimization was performed for 100 ps. The MD simulation was run for 30 ns at 300 K and standard pressure (1.01325 bar) in an orthorhombic box with buffer dimensions of 10 x 10 x 10 Å and an embellished NPT. The energy was recorded at 1.2 ps intervals. Protein-ligand complexes were neutralized by adding Na⁺ or Cl⁻ ions to balance the net charge system of MD simulation. The dynamic Nose-Hoover chain and Martyna-Tobias_klein algorithms were used to maintain the temperature of all MD systems at 300 K and a pressure of 1.01325 bar, respectively [31, 32, 33].

3. Results and Discussion

3.1. Physicochemical Screening of Test Compounds

Pharmacokinetic predictions have been performed using the PreADMET program with the parameters of Caco-2, human intestinal absorption (HIA), and plasma protein binding (PPB), as shown in Table 1. Caco-2 cells have a role as a drug transport pathway through the intestinal epithelium, a derivative of human colon adenocarcinoma. Based on Table 1, it can be seen that natural and test ligands have a moderate ability to penetrate cell membranes because their values are in the range of 4–70 [34]. A compound must have an excellent

ability to penetrate cell membranes to reach the target tissue; hence it can provide good biological activity.

Table 1. Predicted pharmacokinetic properties and toxicity

Compound	Predicted absorption and distribution			Predicted Toxicity		
	Caco-2	HIA	PPB	Ames Test	Carcino mouse	Carcino rat
Natural Ligand	21.5866	90.6145	87.206	Mutagen	Positive	Negative
a	45.3267	94.8868	100.00	Mutagen	Negative	Negative
b	22.1617	94.9346	87.139	Mutagen	Negative	Negative
c	40.4583	94.5528	100	Mutagen	Negative	Negative

HIA parameter relates to the ability of a compound to be absorbed in the body. Drug absorption is the passage of drugs from the application site to the circulatory system. The blood distributes drugs from the body surface or certain parts in the organs to all parts of the body. The results showed that the natural ligands and the test ligands had HIA values in the range of 70–100%, meaning that these compounds could be well absorbed in the body.

The protein can influence the drug's effectiveness in the blood plasma (Plasma Protein Binding). The weaker the drug binding, the more effectively the drug penetrates cell membranes. There are two forms of drugs in the blood: bound and unbound [35]. In Table 1, natural ligands had an excellent distribution ability in the body because they had a PPB of less than 90%, meaning they are weakly bounded. In comparison, the three test ligands had a PPB value of more than 90%, meaning that these ligands are highly bound to plasma proteins. Drugs bound to plasma proteins are inactive, while free or unbound drugs can bind to target receptors and provide biological activity.

Toxicity prediction was conducted to see the level of toxicity of natural and test ligands. The toxicity test used three parameters: the Ames test, carcino mouse, and carcino rat. The Ames test was carried out to assess the potential for mutagenicity that could act as a carcinogen. Ligand compounds as candidates for anticancer drugs in high concentrations are not guaranteed to be safe because they have mutagenic effects.

Table 2. Data on Lipinski's Rule of Five

Compound	Molecular Weight (<500 g/mol)	Hydrogen Donor (<5)	Hydrogen Acceptor (<10)	Log P (<5)	Refractory Molar (40–130)
Natural Ligand	262.735	2	2	2.91	71.97
a	334.519	2	1	6.11	102.72
b	314	2	5	2.14	86.97
c	306.466	2	1	5.22	93.51

The carcino mouse and carcino rat parameters are used to determine whether the ligands can have a carcinogenic effect on rats and mice, the results showed that all the tested ligands did not have a carcinogenic effect on mice or rats. However, the test ligands based on predictions can have a carcinogenic effect on mice. As a result, natural and test ligands as candidates for anticancer drugs possess certain limitations. Besides, it is

supported by Lipinski's Rule of Five rules as listed in Table 2.

The lipophilicity or hydrophobicity of the ligand compound can be determined from the partition coefficient value ($\log P$). A high $\log P$ value indicates that the molecule is hydrophobic. Also, highly hydrophobic molecules increase the risk of toxicity. The test ligand has a higher hydrophobic property because the $\log P$ value is more than 5. Hydrophobic compounds will be retained longer in the lipid bilayer because the layer has hydrophobic properties. Moreover, these compounds will be more widely distributed in the body; therefore, the selectivity of binding to target receptors is reduced [36].

The molecular weight of a compound can affect the drug distribution process by observing its ability to penetrate biological membranes through a passive diffusion process. Compounds with large molecular sizes have a low ability to penetrate biological membranes. The test ligands and natural ligands had a small molecular weight, making them easily penetrate biological membranes.

The parameters of hydrogen bond donor (less than 5) and hydrogen bond acceptor (less than 10) are related to the biological activity of the drug molecule. The presence of hydrogen bonds can affect the physicochemical properties of a compound. The number of hydrogen bond donors in a compound will bond with the solvent to form hydrogen bonds. Likewise, the hydrogen acceptors affect permeability by interacting favorably with a strong hydrogen-bonding solvent. Therefore, compounds that interact with polar solvents can reduce their ability to permeate the lipid bilayer.

The refractory molar values of all ligands met the requirements in the range of 40–130. This value measures the total polarizability of drug molecules that depend on the refractive index, temperature, and pressure.

3.2. Preparation of Ligands and Receptors

At this stage, protonation of the ligand occurs to adjust itself to a blood pH of around 7.4. At the same time, the conformational step was performed to obtain the molecule's position at the lowest or stable energy; thus, it can interact with the receptor's active site. There were ten conformations in the preparation, and one conformation with the lowest energy was continued for the docking process. Receptor preparation was aimed to remove the water content that could block the ligand-receptor interaction [26].

3.3. Molecular Docking Validation

In Figure 2, it can be seen that the results of the re-docking validation of the SIRT1 protein with a grid box size of $40 \times 40 \times 40$ Å and x, y, and z coordinates (42.194; -21,207; and 18,508 Å) against (6S)-2-chloro-

5,6,7,8,9,10-hexahydrocyclohepta[b]indole-6-carboxamide as a natural ligand obtained an RMSD value of 0.374 Å. The overlay image between the crystallographic structure and the re-docking results can be seen in Figure 2.

The valid receptor parameter ($\text{RMSD} < 2$ Å) showed similarity based on comparing the distance change and the best ligand conformation in the simulation results with the initial ligand distance and conformation.

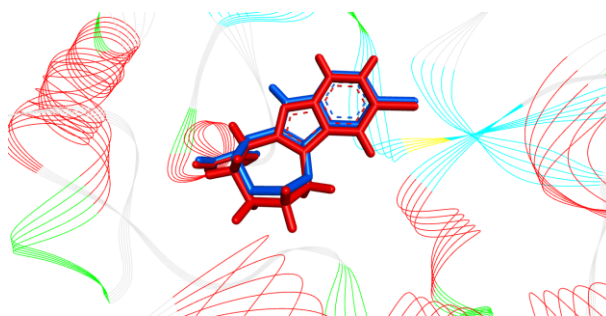


Figure 2. Overlay of natural ligand conformation re-docking results (red) and crystallographic results (blue)

3.4. Docking of Test Ligand

In docking of test ligand stage, the parameters used to determine the binding affinity value are analysis of binding free energy (ΔG) and constant of inhibition (KI). The stability of the interaction between the ligand and the target receptor was predicted with the bond free energy analysis, which was indicated by a low ΔG value [37]. The results can be seen in Table 3, that compound b was predicted to have an activity value of -9.29 kcal/mol, with the resulting inhibition constant value being directly proportional to 0.156 μM . In contrast, the other test ligands had a higher ΔG value, as revealed by compound a of -9.07 kcal/mol and compound c of -8.68 kcal/mol. However, natural ligands were still lower at -9.74 kcal/mol. The low value of ΔG produced leads to a stable ligand-receptor conformation formed.

Table 3. Data on results of molecular docking with SIRT- 1

Compound	Run	ΔG (kcal/mol)	KI (μM)	Hydrogen Bond	Hydrophobic Bond
Natural ligand (d)	68	-9.74	0.073	GlnA:345, IleA:347, AspA:348 (2)	PheA:413, IleA:411, PheA:297, PheA:273, AlaA:262, IleA:279
a	55	-9.07	0.224	HisA:363, ValA:412 (2)	PheA:297, IleA:347, IleA:316, PheA:273, PheA:321, IleA:270, LeuA:350
b	86	-9.29	0.156	AlaA:262, GlnA:345, AsnA:346	PheA:297, IleA:347, IleA:411
c	90	-8.68	0.437	ArgA:274, GlnA:345, SerA:441	AlaA:262, PheA:297, GlyA:440, HisA:363

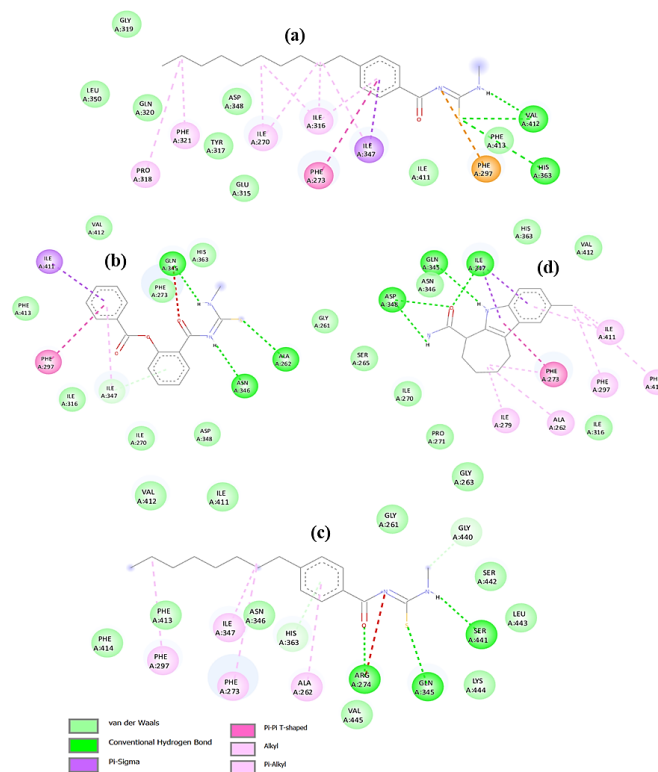


Figure 3. 2D interaction of ligands with amino acid residues: compound a, compound b, compound c, and (d) natural ligand

On the other hand, the ligand–receptor complex is less stable when the ΔG value is high. The more negative the ΔG value leads to the higher affinity of the protein–ligand complex, the stable interaction between the compound and its receptor, and the better the compound activity. The ΔG results will be directly proportional to the KI value, where the KI value describes the ability of the compound to inhibit the enzyme.

3.5. Visualization of the Docking Results

Figure 3 shows 2D interactions between the ligands and amino acid residues (proteins). The closer the distance between the ligand bonds to the amino acid residues on the receptor, the more the ligand bonds with these residues; thus, the more stable the resulting bond.

All thiourea derivatives have three hydrogen interactions with different amino acid residues. In contrast, the natural ligand (d) has four hydrogen bonds because there is an AspA:348 residue that hydrogen interacts with two different groups in the natural ligand. Hydrogen bonding is a desirable bond in ligand–receptor interactions because it can affect the physicochemical properties of compounds and their biological activities. The hydrophobic bond indicates the level of drug solubility in the cell membrane, which is predicted to be effectively bound to the receptor. The presence of hydrogen and hydrophobic bonds in thiourea derivatives and natural ligands is because these compounds have some of the same groups, including C=O, -NH, and a benzene ring.

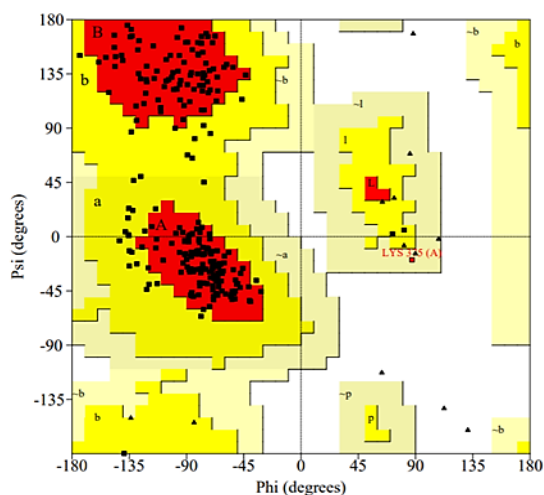
The same amino acid residues on the test ligands and target receptors indicate that the test compounds interact stably with the receptor binding site and have competitive activity. The active site area is the site of protein binding

to ligand compounds involving amino acid residues by forming a stable conformational structure from ligand–receptor interactions. The residues located in the binding side region of the receptor (4I5I.pdb) were IleA:270, ProA:271, AlaA:262, IleA:316, IleA:279, IleA:316, IleA:279, PheA:273, PheA:297, IleA:411, PheA:413, AspA:348, AsnA:346, IleA:347, GlnA:345, HisA:363 and ValA:412.

3.6. Dynamic Molecular Simulation Analysis

Molecular dynamics simulation was conducted on the best-bonded compound (compound b) and natural ligand compounds. Molecular dynamics simulations aimed to discern the stability of the bonded ligand–protein interactions from the docking results. Several factors that influence the results of molecular dynamics simulations include the conformation of compounds, water molecules, ions, cofactors, protonation of compounds, and the conformation of the solvent entropy [31]. Several research results to support the role and importance of molecular dynamics simulation for the refinement of molecular dynamics have been reported. The final structure of the molecular dynamics simulation of compound b showed a stable stereochemical geometry, as shown in the analysis of the Ramachandran plot of Figure 4.

Based on the Ramachandran plot, the percent residues in favored, allowed, and disallowed regions of the b–SIRT1 compound complex can also be observed in Figure 4. From Figure 4, it can be explained that the b–SIRT1 complex is gemlike residue in the favored region was around 84.4%, and there was no residue in the disallowed region. In conclusion, the quality of the b–SIRT1 complex was excellent.



Plot statistics

Residues in most favoured regions [A,B,L]	198	84.3%
Residues in additional allowed regions [a,b,l,p]	36	15.3%
Residues in generously allowed regions [-a,-b,-l,-p]	1	0.4%
Residues in disallowed regions	0	0.0%
Number of non-glycine and non-proline residues	235	100.0%
Number of end-residues (excl. Gly and Pro)	2	
Number of glycine residues (shown as triangles)	14	
Number of proline residues	21	
Total number of residues	272	

Figure 4. Ramachandran plot of compound b

Based on the Ramachandran plot, the percent residues in favored, allowed, and disallowed regions of the b-SIRT1 compound complex can also be observed in Figure 4. From Figure 4, it can be explained that the b-SIRT1 complex is gemlike residue in the favored region was around 84.4%, and there was no residue in the disallowed region. In conclusion, the quality of the b-SIRT1 complex was excellent.

In addition, the stability of the complex interaction of the b-SIRT1 compound can also be seen from the graph of the RMSD during a 30 ns simulation, as shown in Figure 5.

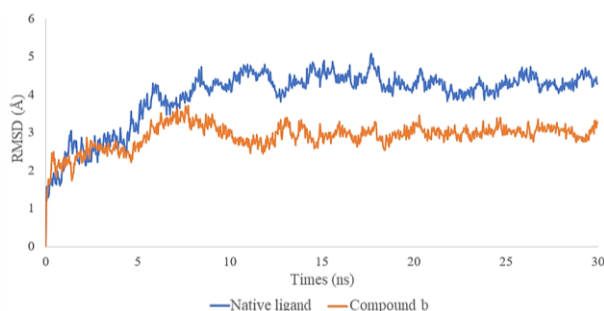


Figure 5. RMSD plot of the ligand-SIRT1 complex: compound b-SIRT1 (orange) and natural ligand-SIRT1 (blue)

Based on the RMSD graph, the complex b-SIRT1 and natural ligand-SIRT1 have a fluctuating RMSD from 0–14 ns, then after 14 ns until the end of the simulation, 30 ns has a reasonably stable RMSD. From the RMSD graph, it can be concluded that for 30 ns of molecular dynamics simulation, the complex with the most stable interaction stability is the b-SIRT1 complex compared to the natural ligand-SIRT1 complex. This result is supported by the average, minimum and maximum values of RMSD during the 30 ns simulation of each SIRTUIN1-ligand complex, as shown in Table 4.

Table 4. Average, minimum, and maximum value of RMSD ligand-protein complex

Complex System	Average	Minimum	Maximum
Compound b-SIRT1	2.898	1.176	3.703
Natural ligand-SIRT1	3.975	1.05	5.073

Besides RMSD, interaction stability was also evaluated using the RMSF graph, shown in Figure 6.

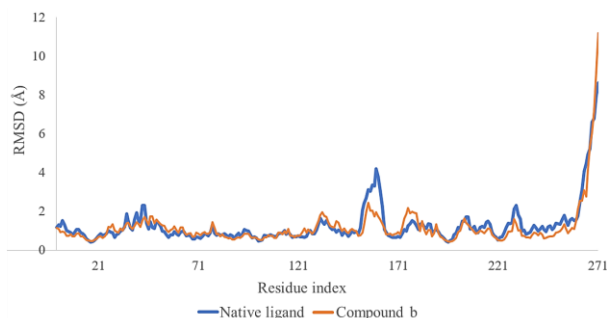


Figure 6. RMSF graph of the complex system of compound b-SIRT1 (orange) and natural ligand-SIRT1 (blue)

According to the RMSF graph, the SIRT1-ligand can be used to prove the stability of the interaction. It is illustrated that the fluctuations of the residues have fluctuations in the same area. Still, the complex system of b-SIRT1 compounds has lower fluctuations than the natural ligand-SIRT1 if seen from the average RMSF of the compound-complex b-SIRT1 (1.163 Å) and natural ligand-SIRT1 (1.255 Å). The graph proves that the complex system of b-SIRT1 is a more stable interaction than the natural ligand-SITR1 complex system.

The RMSF graphic analysis can also identify amino acid residues that have contact/interaction with the ligand, as shown in Figure 7. Figure 7 shows the RMSF fluctuation and the residues that contact compound b.

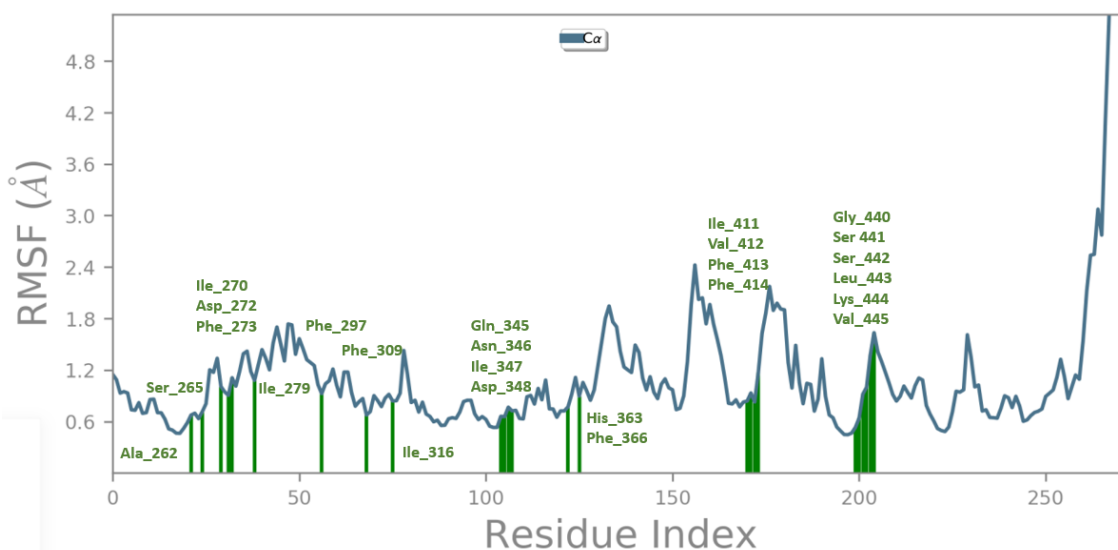


Figure 7. Graph of RMSF and the residues contact in the complex system of b-SIRT1 compounds at a simulated MD of 30 ns

From Figure 7, it can be explained that the residues that have contact/interaction with compound **b** are Ala_262, Ser_265, Ile_270, Asp_272, Phe_273, Ile_279, Phe_297, Phe_305, Ile_316, Gln_345, Asn_346, Ile_347, His_363, Ile_411, Val_412, Phe_413, Phe_414, Gly_440, Ser_441, Ser_442, Leu_443, Lys_444 and Val_445 (25 contact residues) both interacting through hydrogen bonds, hydrophobic bonds, ionic and water bridges, as shown in Figure 7 and Figure 8.

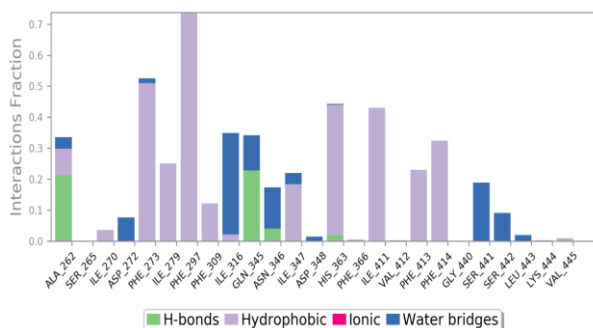


Figure 8. Residue contact diagram of the compound b-SIRT1 complex

Figure 9 shows that the residues interact with the ligands at each pass. Some protein residues showed more than one specific contact with the ligand, which marked a darker orange color. Overall, six parameters were analyzed to explain the stability of compound **b** at the SIRT1 receptor during the 30 ns MD simulation, as depicted in Figure 10.

Figure 10 shows that the simulation process of compound **b** RMSD fluctuated. In the early stages, fluctuations were observed from 0 to 17 ns, and after that, constant RMSD was observed during the whole simulation process. Fluctuations for gyration's radius were recorded up to 17 ns, and further, a stable conformation was obtained until the end of the simulation. The simulation radius of 30 ns of gyration ranged from 3.371 to 3.948 for compound **b**. The SASA plot revealed a fluctuating pattern for 3 ns and stabilized until the simulation was complete. MolSA and PSA plots for compound **b** up to 17 ns fluctuated but remained stable until the end of the 30 ns simulation. Meanwhile, the plot of the intramolecular H-bond of compound **b**, from the beginning to the end of the simulation, showed the intramolecular H-bond, which became stable after protein interactions.

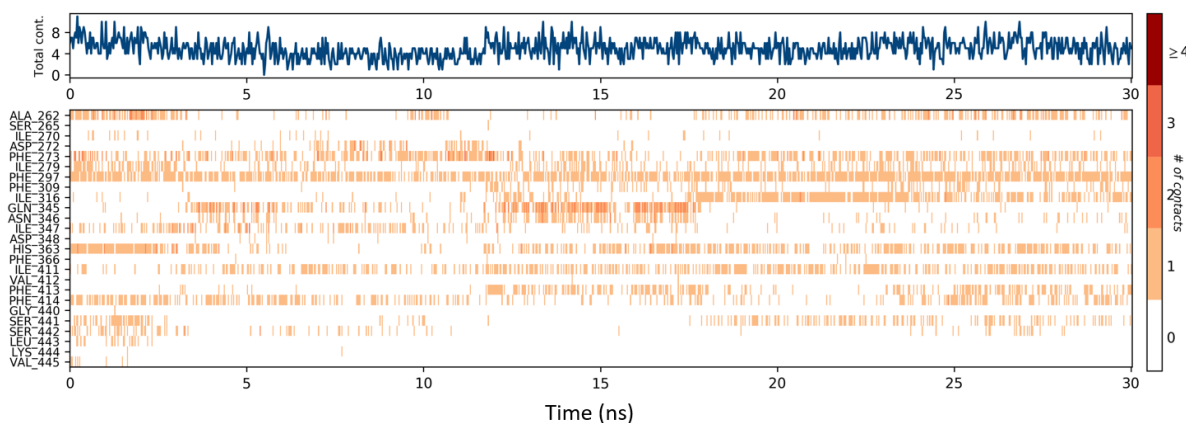


Figure 9. Representation of residue contacts and interactions of b-SIRT1 compounds during MD 30 ns

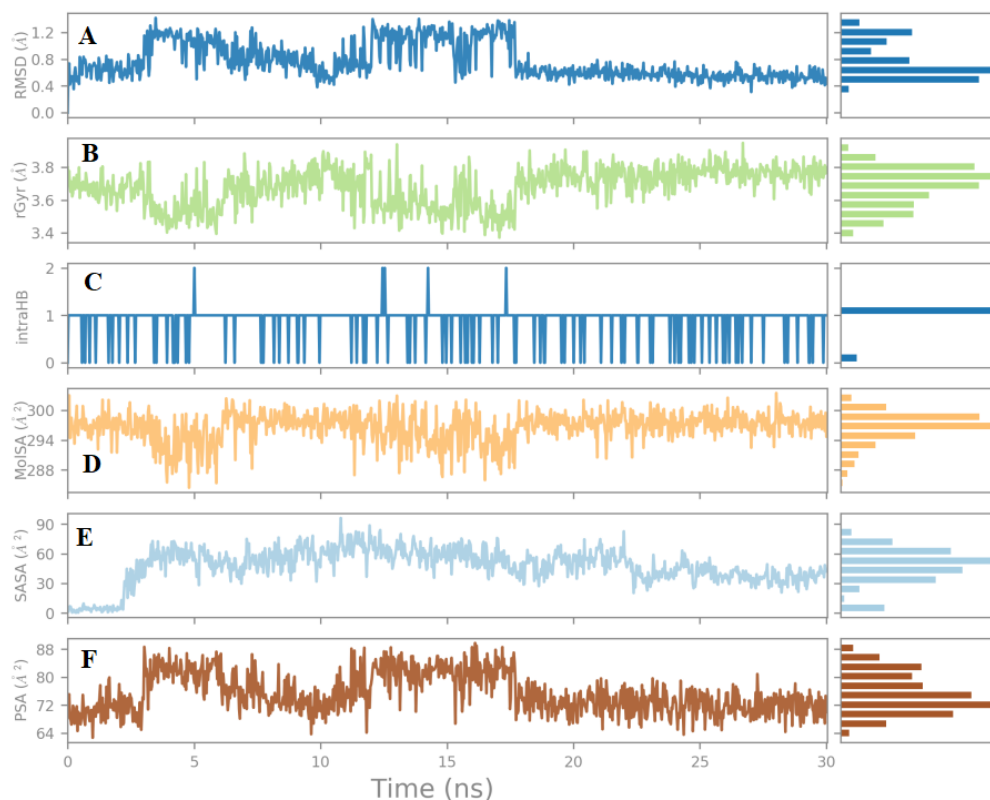


Figure 10. Characterization of compound **b** during the 30 ns MD simulation: (A) ligand RMSD, (B) radius of gyration (rGyr), (C) NS34, (D) molecular surface area (MolSA), (E) solvent accessible surface area (SASA), and (F) polar surface area (PSA)

Figure 10 shows that the simulation process of compound **b** RMSD fluctuated. In the early stages, fluctuations were observed from 0 to 17 ns, and after that, constant RMSD was observed during the whole simulation process. Fluctuations for gyration's radius were recorded up to 17 ns, and further, a stable conformation was obtained until the end of the simulation. The simulation radius of 30 ns of gyration ranged from 3.371 to 3.948 for compound **b**. The SASA plot revealed a fluctuating pattern for 3 ns and stabilized until the simulation was complete. MolSA and PSA plots for compound **b** up to 17 ns fluctuated but remained stable until the end of the 30 ns simulation. Meanwhile, the plot of the intramolecular H-bond of compound **b**, from the beginning to the end of the simulation, showed the intramolecular H-bond, which became stable after protein interactions.

3D visualization of compound **b** complex and natural ligand with SIRT1 after 30 ns simulation is illustrated in Figure 11.

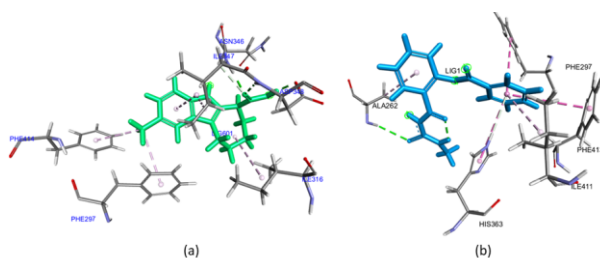


Figure 11. (a) The complex of natural ligand–SIRT1 (6), (b) **b**–SIRT1 compound complex at the end of the 30 ns MD simulation

From Figure 10, it can be seen that the Phe_297 residue interacts with both natural ligands and with compound **b** following the results of the research in the reference that Phe_297 is one of the amino acid residues that interact with compound **415** ((6S)-2-chloro-5,6,7,8,9,10-hexahydrocyclohepta[b]indole-6-carboxamide) [25].

4. Conclusion

From the molecular docking results, it was concluded that compound **b** ([2-(methylcarbamothioylcarbamoyl)phenyl]benzoate) had the lowest ΔG value of -9.29 kcal/mol with a KI value of $0.156 \mu\text{M}$ compared to the other two thioureas, supported by the result of molecular dynamics simulation for 30 ns. The active site amino acid residue that interacts with the ligand is PheA:297. In terms of pharmacokinetics and toxicity of compound **b** is better than natural ligands, it can be concluded that compound **b** is predicted to be conducted further research as an anticancer candidate through inhibition of SIRT1.

Acknowledgment

Researchers would like to thank the Ministry of Education, Culture, Research, and Technology for the Post-Doctoral Research Grant (NKB-/UN2.RST/HKP.05.00/2021).

References

- [1] World Health Organization, *Cancer*, World Health Organization, 2021
- [2] J. Ferlay, M. Ervik, F. Lam, M. Colombet, L. Mery, *Global Cancer Observatory: Cancer Today*,

- International Agency for Research on Cancer, World Health Organization, 2020
- [3] Kementerian Kesehatan Republik Indonesia, in, Pusat Data dan Informasi Kementerian Kesehatan Republik Indonesia, Jakarta, 2015,
 - [4] Birsan Elibol, Ulkan Kilic, High levels of SIRT1 expression as a protective mechanism against disease-related conditions, *Frontiers in Endocrinology*, 9, 614, (2018), 1-7 <https://doi.org/10.3389/fendo.2018.00614>
 - [5] Zhenghong Lin, Deyu Fang, The roles of SIRT1 in cancer, *Genes & Cancer*, 4, 3-4, (2013), 97-104 <https://doi.org/10.1177/1947601912475079>
 - [6] Wenwen Zang, Yujun Hao, Zhenghe Wang, Weiping Zheng, Novel thiourea-based sirtuin inhibitory warheads, *Bioorganic & Medicinal Chemistry Letters*, 25, 16, (2015), 3319-3324 <https://doi.org/10.1016/j.bmcl.2015.05.058>
 - [7] Carmen Avendaño, J. Carlos Menendez, *Medicinal chemistry of anticancer drugs*, 2nd ed., Elsevier, Netherlands, 2015
 - [8] Pillaiyar Thanigaimalai, Ki-Cheul Lee, Vinay K. Sharma, Cheonik Joo, Won-Jea Cho, Eunmiri Roh, Youngsoo Kim, Sang-Hun Jung, Structural requirement of phenylthiourea analogs for their inhibitory activity of melanogenesis and tyrosinase, *Bioorganic & Medicinal Chemistry Letters*, 21, 22, (2011), 6824-6828 <https://doi.org/10.1016/j.bmcl.2011.09.024>
 - [9] Ali Sohail Farooqi, Jun Young Hong, Ji Cao, Xuan Lu, Ian Robert Price, Qingjie Zhao, Tatsiana Kosciuk, Min Yang, Jessica Jingyi Bai, Hening Lin, Novel lysine-based thioureas as mechanism-based inhibitors of Sirtuin 2 (SIRT2) with anticancer activity in a colorectal cancer murine model, *Journal of Medicinal Chemistry*, 62, 8, (2019), 4131-4141 <https://doi.org/10.1021/acs.jmedchem.9b00191>
 - [10] Dini Kesuma, Bambang Tri Purwanto, Marcellino Rudyanto, Synthesis and anticancer evaluation of N-benzoyl-N'-phenylthiourea derivatives against human breast cancer cells (T47D), *Journal of Chinese Pharmaceutical Sciences*, 29, 2, (2019), 123-129 <http://dx.doi.org/10.5246/jcps.2020.02.010>
 - [11] Suko Hardjono, Tri Widiandani, Bambang Tri Purwanto, Anindi L. Anindi, Molecular docking of N-benzoyl-N'-(4-fluorophenyl) thiourea derivatives as anticancer drug candidate and their ADMET prediction, *Research Journal of Pharmacy and Technology*, 12, 5, (2019), 2160-2166 <http://dx.doi.org/10.5958/0974-360X.2019.00359.7>
 - [12] Dini Kesuma, Harry Santosa, Sintesis Senyawa 2, 4-diklorobenzoiltiourea dari 2, 4-diklorobenzoil klorida dan Tiourea Sebagai Calon Obat Central Nervous System Depressant Melalui Proses Refluks, *Seminar Nasional Teknik Kimia Indonesia*, Bandung, 2009
 - [13] Fatma Karipcin, Murat Atis, Bahtiyar Sariboga, Hasan Celik, Murat Tas, Structural, spectral, optical and antimicrobial properties of synthesized 1-benzoyl-3-furan-2-ylmethyl-thiourea, *Journal of Molecular Structure*, 1048, (2013), 69-77 <https://doi.org/10.1016/j.molstruc.2013.05.042>
 - [14] Wukun Liu, Jinpei Zhou, Tong Zhang, Haiyang Zhu, Hai Qian, Huibin Zhang, Wenlong Huang, Ronald Gust, Design and synthesis of thiourea derivatives containing a benzo [5, 6] cyclohepta [1, 2-b]pyridine moiety as potential antitumor and anti-inflammatory agents, *Bioorganic & Medicinal Chemistry Letters*, 22, 8, (2012), 2701-2704 <https://doi.org/10.1016/j.bmcl.2012.03.002>
 - [15] G. Kirishnamaline, J. Daisy Magdaline, T. Chithambarathanu, D. Aruldas, A. Ronaldo Anuf, Theoretical investigation of structure, anticancer activity and molecular docking of thiourea derivatives, *Journal of Molecular Structure*, 1225, 129118, (2021), 1-24 <https://doi.org/10.1016/j.molstruc.2020.129118>
 - [16] Harry Santosa, Dini Kesuma, Aktivitas Antikanker Senyawa N-Etil-N-Feniltiourea secara In Silico dan In Vitro Pada Sel Kanker Payudara T47D dan Selektivitasnya pada Sel Normal Vero, *Kongres XX & Pertemuan Ilmiah Tahunan Ikatan Apoteker Indonesia*, Jakarta, 2018
 - [17] Reem A. K. Al-Harbi, Marwa A.M. Sh. El-Sharief, Samir Y. Abbas, Synthesis and anticancer activity of bis-benzo [d][1, 3] dioxol-5-yl thiourea derivatives with molecular docking study, *Bioorganic Chemistry*, 90, (2019), 1-9 <https://doi.org/10.1016/j.bioorg.2019.103088>
 - [18] Bachwani Mukesh, Kumar Rakesh, Molecular docking: a review, *International Journal of Research in Ayurveda & Pharmacy*, 2, 6, (2011), 1746-1751
 - [19] Md. Mushtaque, Meriyam Jahan, Murtaza Ali, Md Shahzad Khan, Mohd Shahid Khan, Preeti Sahay, Ashwani Kesarwani, Synthesis, characterization, molecular docking, DNA binding, cytotoxicity and DFT studies of 1-(4-methoxyphenyl)-3-(pyridine-3-ylmethyl) thiourea, *Journal of Molecular Structure*, 1122, (2016), 164-174 <https://doi.org/10.1016/j.molstruc.2016.05.087>
 - [20] Tero Huhtiniemi, Tiina Suuronen, Valtteri M. Rinne, Carsten Wittekindt, Maija Lahtela-Kakkonen, Elina Jarho, Erik A. A. Wallén, Antero Salminen, Antti Poso, Jukka Leppanen, Oxadiazole-carbonylaminothioureas as SIRT1 and SIRT2 inhibitors, *Journal of Medicinal Chemistry*, 51, 15, (2008), 4377-4380 <https://doi.org/10.1021/jm800639h>
 - [21] Ruswanto Ruswanto, Richa Mardianingrum, Tresna Lestari, Tita Nofianti, Siswandono Siswandono, 1-(4-Hexylbenzoyl)-3-methylthiourea, *Molbank*, 2018, 3, (2018), <https://doi.org/10.3390/M1005>
 - [22] Ruswanto Ruswanto, Amir M. Miftah, Daryono H. Tjahjono, Siswandono Siswandono, In silico study of 1-benzoyl-3-methylthiourea derivatives activity as epidermal growth factor receptor (EGFR) tyrosine kinase inhibitor candidates, *Chemical Data Collections*, 34, 100741, (2021), 1-33 <https://doi.org/10.1016/j.cdc.2021.100741>
 - [23] Amir M. Miftah, Daryono H. Tjahjono, Synthesis and in vitro Cytotoxicity of 1-Benzoyl-3-methyl Thiourea Derivatives, *Procedia Chemistry*, 17, (2015), 157-161 <https://doi.org/10.1016/j.proche.2015.12.105>
 - [24] David S. Goodsell, Garrett M. Morris, Arthur J. Olson, Automated docking of flexible ligands: applications of AutoDock, *Journal of Molecular Recognition*, 9, 1, (1996), 1-5 [https://doi.org/10.1002/\(SICI\)1099-1352\(199601\)9:1<1::AID-JMR241>3.0.CO;2-6](https://doi.org/10.1002/(SICI)1099-1352(199601)9:1<1::AID-JMR241>3.0.CO;2-6)

- [25] Xun Zhao, Dagart Allison, Bradley Condon, Feiyu Zhang, Tarun Gheyi, Aiping Zhang, Sheela Ashok, Marijane Russell, Iain MacEwan, Yuewei Qian, The 2.5 Å crystal structure of the SIRT1 catalytic domain bound to nicotinamide adenine dinucleotide (NAD⁺) and an indole (EX527 analogue) reveals a novel mechanism of histone deacetylase inhibition, *Journal of Medicinal Chemistry*, 56, 3, (2013), 963–969 <https://doi.org/10.1021/jm301431y>
- [26] Ruswanto Ruswanto, Richa Mardianingrum, Siswandono Siswandono, Dini Kesuma, Reverse docking, molecular docking, absorption, distribution, and toxicity prediction of artemisinin as an anti-diabetic candidate, *Molekul*, 15, 2, (2020), 88–96 <https://doi.org/10.20884/1.jm.2020.15.2.579>
- [27] Richa Mardianingrum, Sri Rezeki Nur Endah, Eddy Suhardiana, Ruswanto Ruswanto, Siswandono Siswandono, Docking and molecular dynamic study of isoniazid derivatives as anti-tuberculosis drug candidate, *Chemical Data Collections*, 32, 100647, (2021), 1–11 <https://doi.org/10.1016/j.cdc.2021.100647>
- [28] Ruswanto Ruswanto, Mardhiah Mardhiah, Richa Mardianingrum, Korry Novitriani, Sintesis dan Studi *In Silico* Senyawa 3-Nitro-N'-[(Pyridin-4-Yl) Carbonyl] Benzohydrazide sebagai Kandidat Antituberkulosis, *Chimica et Natura Acta*, 3, 2, (2015), 54–61 <https://doi.org/10.24198/cna.v3.n2.9183>
- [29] Karisma Enggar Saputri, Nurul Fakhmi, Erwinda Kusumaningtyas, Dedy Priyatama, Broto Santoso, Docking molekular potensi anti diabetes melitus tipe 2 turunan zerumbon sebagai inhibitor aldosa reduktase dengan autodock-vina, *Chimica et Natura Acta*, 4, 1, (2016), 16–20 <https://doi.org/10.24198/cna.v4.n1.10443>
- [30] Oleg Trott, Arthur J. Olson, AutoDock Vina: improving the speed and accuracy of docking with a new scoring function, efficient optimization, and multithreading, *Journal of Computational Chemistry*, 31, 2, (2010), 455–461 <https://doi.org/10.1002/jcc.21334>
- [31] Sumit Kumar, Prem Prakash Sharma, Uma Shankar, Dhruv Kumar, Sanjeev K. Joshi, Lindomar Pena, Ravi Durvasula, Amit Kumar, Prakasha Kempaiah, Poonam, Discovery of new hydroxyethylamine analogs against 3CL^{pro} protein target of SARS-CoV-2: Molecular docking, molecular dynamics simulation, and structure–activity relationship studies, *Journal of Chemical Information and Modeling*, 60, 12, (2020), 5754–5770 <https://doi.org/10.1021/acs.jcim.0c00326>
- [32] Larisa Ivanova, Jaana Tammiku-Taul, Alfonso T. García-Sosa, Yulia Sidorova, Mart Saarma, Mati Karelson, Molecular dynamics simulations of the interactions between glial cell line-derived neurotrophic factor family receptor GFR α 1 and small-molecule ligands, *ACS Omega*, 3, 9, (2018), 11407–11414 <https://doi.org/10.1021/acsomega.8b01524>
- [33] Chetan Chintha, Antonio Carlesso, Adrienne M. Gorman, Afshin Samali, Leif A. Eriksson, Molecular modeling provides a structural basis for PERK inhibitor selectivity towards RIPK1, *RSC Advances*, 10, 1, (2020), 367–375 <https://doi.org/10.1039/C9RA08047C>
- [34] Nursalam Hamzah, Afrisusnawati Rauf, Ariwanti Ariwanti, Studi hubungan kuantitatif struktur-aktifitas (hkksa) senyawa turunan 4-aminoquinolin pirimidin, docking molekul, penelusuran farmakofor, virtual screening, uji toksisitas, dan profil farmakokinetik sebagai antimalaria secara *in silico*, *Jurnal Farmasi UIN Alauddin Makassar*, 3, 4, (2017), 176–186
- [35] Nursamsiar Nursamsiar, Alprida Tandi Toding, Akbar Awaluddin, Studi *in silico* senyawa turunan analog kalkon dan pirimidin sebagai antiinflamasi: Prediksi absorpsi, distribusi, dan toksisitas, *Pharmacy: Jurnal Farmasi Indonesia (Pharmaceutical Journal of Indonesia)*, 13, 1, (2016), 92–100
- [36] Gita Syahputra, L. Ambarsari, T. Sumaryada, Simulasi docking kurkumin enol, bisdemetoksikurkumin dan analognya sebagai inhibitor enzim 12-lipoksigenase, *Jurnal Biofisika*, 10, 1, (2014), 55–67
- [37] Richa Mardianingrum, Muhammad Yusuf, Maywan Hariono, Amira Mohd Gazzali, Muchtaridi Muchtaridi, α -Mangostin and its derivatives against estrogen receptor alpha, *Journal of Biomolecular Structure and Dynamics*, (2020), 1–14 <https://doi.org/10.1080/07391102.2020.1841031>